ORIGINAL RESEARCH

Evaluation of Aqueductal Stenosis by 3D Sampling Perfection with Application-Optimized Contrasts Using Different Flip Angle Evolutions Sequence: Preliminary Results with 3T MR Imaging

O. Algin
B. Turkbey

BACKGROUND AND PURPOSE: Diagnosis of AS and periaqueductal abnormalities by routine MR imaging sequences is challenging for neuroradiologists. The aim of our study was to evaluate the utility of the 3D-SPACE sequence with VFAM in patients with suspected AS.

MATERIALS AND METHODS: PC-MRI and 3D-SPACE images were obtained in 21 patients who had hydrocephalus on routine MR imaging scans and had clinical suspicion of AS, as well as in 12 control subjects. Aqueductal patency was visually scored (grade 0, normal; grade 1, partial obstruction; grade 2, complete stenosis) by 2 experienced radiologists on PC-MRI (plus routine T1-weighted and T2-weighted images) and 3D-SPACE images. Two separate scores were statistically compared with each other as well as with the consensus scores obtained from general agreement of both radiologists.

RESULTS: There was an excellent correlation between 3D-SPACE and PC-MRI scores ($\kappa = 0.828$). The correlation between 3D-SPACE scorings and consensus-based scorings was higher compared with the correlation between PC-MRI and consensus-based scorings ($r = 1$, $P < .001$ and $r = 0.966$, $P < .001$, respectively).

CONCLUSIONS: 3D-SPACE sequence with VFAM alone can be used for adequate and successful evaluation of the aqueductal patency without the need for additional sequences and examinations. Noninvasive evaluation of the whole cranium is possible in a short time with high resolution by using 3D-SPACE.

ABBREVIATIONS: 3D-CISS = 3D constructive interference in steady state; 3D-SPACE = 3D sampling perfection with application-optimized contrasts using different flip angle evolutions; AS = aqueductal stenosis; CE-MRC = contrast-enhanced MR cisternography; GRAPPA = generalized autocalibrating partially parallel acquisition; MPRAGE = magnetization-prepared rapid acquisition of gradient echo; PC = phase-contrast cine; VFAM = variant flip angle mode

AS is the most common cause of the obstructive hydrocephalus.[1] The etiology of AS is frequently idiopathic, but in some patients, X-linked recessive inheritance has been reported.[2,3] Webbing, adhesion, or aqueductal forking can be listed among etiologic factors of primary non-neoplastic AS.[4] Periaqueductal lesions (such as cysts, tumors, infections) can lead to aqueductal stenosis as well.[2,3] There is no worldwide accepted MR imaging protocol for the evaluation of patients with a preliminary diagnosis of AS; hence, it is usually difficult to clearly define the etiology of hydrocephalus by using routine MR images.[3,5] Moreover, invasive techniques (ie, contrast-enhanced cisternography and/or ventriculographic studies) are required for an accurate diagnosis, and this requirement can easily delay the patient management, increase the cost, and lead to serious complications including death.[3,6]

Received June 19, 2011; accepted after revision July 13.

From Department of Radiology (O.A.), Atatürk Training and Research Hospital, Bilkent, Ankara, Turkey; and National Cancer Institute (B.T.), National Institutes of Health, Bethesda, Maryland 06800.

This study was presented as a scientific poster presentation at the 16th Turkish Society of Magnetic Resonance Annual Meeting, Istanbul, Turkey, May 19–21, 2011.

Please address correspondence to Oktay Algin, MD, Department of Radiology, Atatürk Training and Research Hospital, Bilkent, Ankara, Turkey; e-mail: droktayalgin@gmail.com

http://dx.doi.org/10.3174/ajnr.A2833

In most patients, MR imaging plays a pivotal role in planning the surgical procedure (such as ventriculoperitoneal shunt, endoscopic third ventriculostomy, or endoscopic aqueductoplasty).[3,6,7] With the advent of 3T MR imaging systems, there has been a marked increase in the SNR of images, resulting in improvement of the image quality and spatial resolution and shortening of the scanning times.[8] On the other hand, the main disadvantage of 3T MR imaging systems is their high SAR, which could be eliminated by recently developed approaches such as the 3D-SPACE technique.[9,10] Moreover, using a different flip angle–mode technique at 3T can provide 3D images that can evaluate the whole cranium by shortening the acquisition time.[8] T1-weighted, proton-density weighted, FLAIR, conventional, and/or heavily T2-weighted MR images can be obtained with a high SNR value in a short time and with a low specific absorption rate value with 3D-SPACE.[10] Isotropic 3D acquisitions with high spatial resolution have an important advantage for the evaluation of intracranial complex structures.[11,12]

Our previous experience in animal studies with VFAM instead of a constant flip angle mode in T2-weighted 3D-SPACE sequences revealed a better assessment of CSF flow dynamics as well as a better understanding of the aqueductal patency and definition of the accompanying abnormalities.[13] Our aim in

Table 1: The demographic and clinical characteristics and MRI scores of the patient group

No.	Sex	Age (yr)	PC-MRI	SPACE	Consensus Results	EH	Additional Illness
1	M	7	2	2	2	Web-synechia	NF-1
2	F	61	0	0	0	Idiopathic	DWM
3	M	59	0	0	0	Idiopathic	DWM
4	M	18	0	0	0	FVOO	–
5	F	69	0	0	0	TVAC	–
6	F	57	0	0	0	CoH	DWM
7	F	63	0	0	0	Idiopathic	–
8	M	69	0	0	0	Idiopathic	–
9	M	27	2	2	2	Web	–
10	F	50	2	2	2	Web	–
11	M	40	2	2	2	TG	–
12	M	35	1	1	1	TG	–
13	M	25	2	2	2	Idiopathic	–
14	F	54	0	0	0	FVOO	Chiari1
15	M	62	0	0	0	Idiopathic	–
16	F	34	1	2	2	TG	–
17	M	24	0	0	0	Idiopathic	NF-1
18	M	46	0	0	0	Idiopathic	–
19	F	43	2	1	1	Web	–
20	M	21	0	0	0	Idiopathic	–
21	M	9	2	2	2	Web, gliosis	NF-1

Note:—DWM indicates Dandy-Walker malformation; FVOO, fourth ventricular outlet obstruction; TVAC, third ventricular arachnoid cyst; CoH, complex hydrocephalus; NF-1, neurofibromatosis type 1; EH, etiology of hydrocephalus; TG, tectal glioma.

this prospective study was to evaluate the efficacy of T2-weighted 3D-SPACE with VFAM acquisition in the evaluation of aqueductal patency on a 3T MR imaging system. To the best of our knowledge, there is no previous report in the literature regarding the role of this new sequence in the assessment of aqueductal patency as well as in obstructive hydrocephalus.

Materials and Methods

Study Population

This institutional review board–approved Health Insurance Portability and Accountability Act–compliant study included 28 patients who were referred to our radiology clinic for MR imaging evaluation for hydrocephalus and clinical or radiological suspicion AS between January 2010 and March 2011. Four patients were excluded because their PC-MRI examinations were not evaluable due to technical insufficiency, and 3 patients were excluded due to significant motion artifacts obscuring scan evaluation. The final study population included 21 patients (13 males, 8 females; mean, 34 ± 5 years of age; range, 7–69 years), whereas the control group included 12 healthy volunteers (6 females, 6 males; mean, 32 ± 5 years of age; range, 9–64 years).

MR Imaging Protocol

All MR imaging examinations were performed at a 3T MR imaging system (Trio; Siemens, Erlangen, Germany) by using an 8-channel

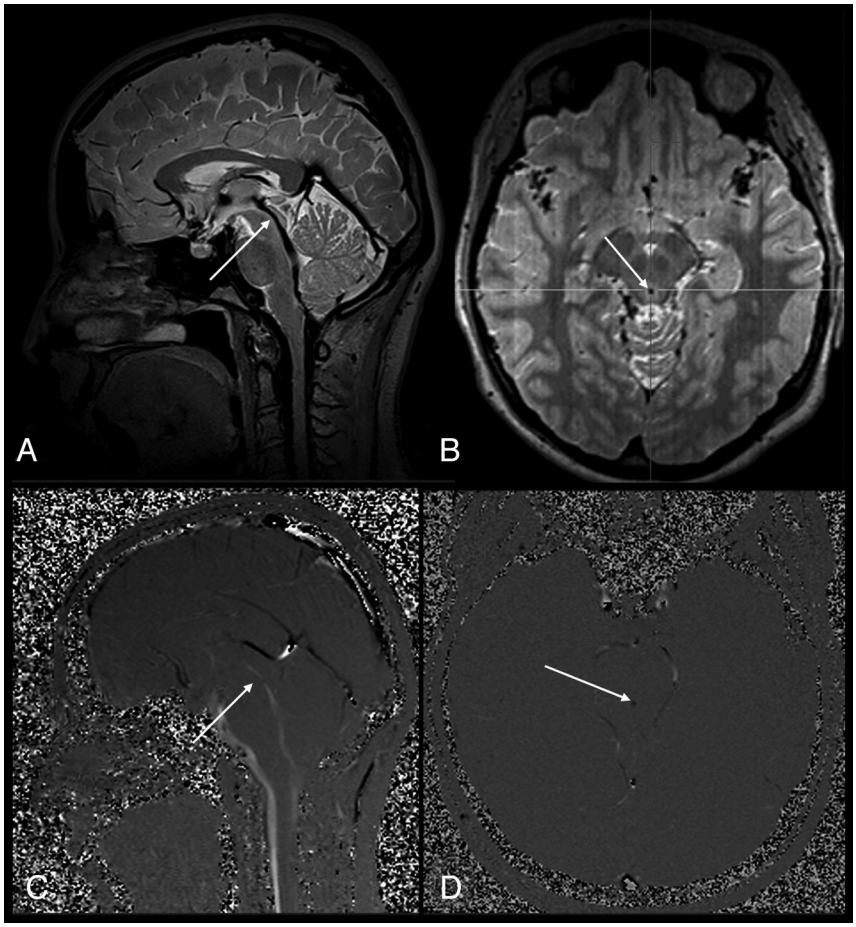

Fig 1. A 23-year-old woman (control). *A*, Sagittal 3D-SPACE with VFAM image shows a normal aqueduct (grade 0, *arrow*). *B*, Thin-section axial reformatted 3D-SPACE with VFAM image demonstrates hypointense flow-void signal intensity consistent with an open aqueduct (*arrow*). *C* and *D*, Sagittal (*C*) and axial (*D*) PC-MRI are well-matched with 3D-SPACE sequence results (*arrows*).

Table 2: The agreement level in consensus-based scores versus PC-MRI and SPACE scores

Consensus Versus	κ	Confidence Interval (95%)	Agreement Level (No.) (%)
PC-MRI	0.828	(0.618–1.000)	19 (90.48)[a]
SPACE	1.000	(1.000–1.000)	21 (100)[a]

[a] The number of times that tests agreed among themselves.

head array coil. All patients and control subjects were scanned in the supine position, and MR imaging protocol parameters are summarized below.

After acquisition of scout images, sagittal plane 3D T1-weighted data were obtained by using an MPRAGE sequence (TR/TE/TI, 2300/3.15/1000 ms; section thickness, 0.8 mm; voxel size, 0.8 × 0.8 × 0.8 mm; FOV, 256 × 256 mm; NEX, 1; distance factor, 50%; number of sections, 240; flip angle, 8°; parallel acquisition techniques, 2; parallel acquisition techniques mode, GRAPPA; acquisition time, 5.57 minutes). Then, a 3-plane 2D T2-weighted TSE sequence (TR/TE, 6000/93 ms; section thickness, 3 mm; FOV, 220 × 220 mm; NEX, 1; distance factor, 30%; flip angle, 120°; parallel acquisition techniques, 2; parallel acquisition techniques mode, GRAPPA; 1.26 minutes) and sagittal-axial plane flow-compensated spoiled gradient-echo PC-MRI technique (2D fast imaging with steady-state precession sequence) with retrospective cardiac gating were obtained with the following parameters: TR/TE, 34.9/9.8 ms; FOV, 240 × 240 mm; section thickness, 4 mm; NEX, 2; parallel acquisition techniques, none; section number, 1; flip angle, 10°; section thickness, 4 mm; FOV, 160 mm; NEX, 1; velocity encoding, 6 cm/s. Twenty-four magnitude-phase and rephased images were obtained from every PC-MRI sequence. The PC-MRI sequence image-acquisition time was approximately 5 minutes, though heart rate was a determining factor.

After acquisition of T1-weighted, T2-weighted, and PC-MRI, a 3D-SPACE sequence with isotropic voxel size (0.6 × 0.6 × 0.6 mm) was obtained in the sagittal plane. Sequence parameters of 3D-SPACE were as follows: TR/TE, 3000/579; FOV, 275 × 275 mm; NEX, 2; sections per slab, 208; parallel acquisition techniques, 2; parallel acquisition techniques mode, GRAPPA; echo spacing, 3.34 ms; turbo factor, 173; section turbo factor, 2; flip angle mode, T2 variant (VFAM); acquisition time, 6.24 minutes.

Volumetric data obtained from 3D T1-weighted and 3D-SPACE sequences was transferred to dedicated workstations (Leonardo, Siemens) of the MR imaging unit, and thin-section reformatted (coronal, axial, and oblique planes) maximum intensity projection images were achieved.

3D T1-weighted and 3D-SPACE images were evaluated independently by 2 different experienced radiologists in different workstations with the same display configuration and settings (Leonardo, Siemens). The presence of AS and accompanying findings was recorded without checking routine T2-weighted and PC-MRI. Aqueductal patency was scored visually as described below.

Score Zero (AS-Negative). The aqueduct is within normal ranges, and there is no evidence of an intraluminal abnormality. There is a hypointense CSF flow from third ventricle toward the fourth ventricle through the aqueduct.

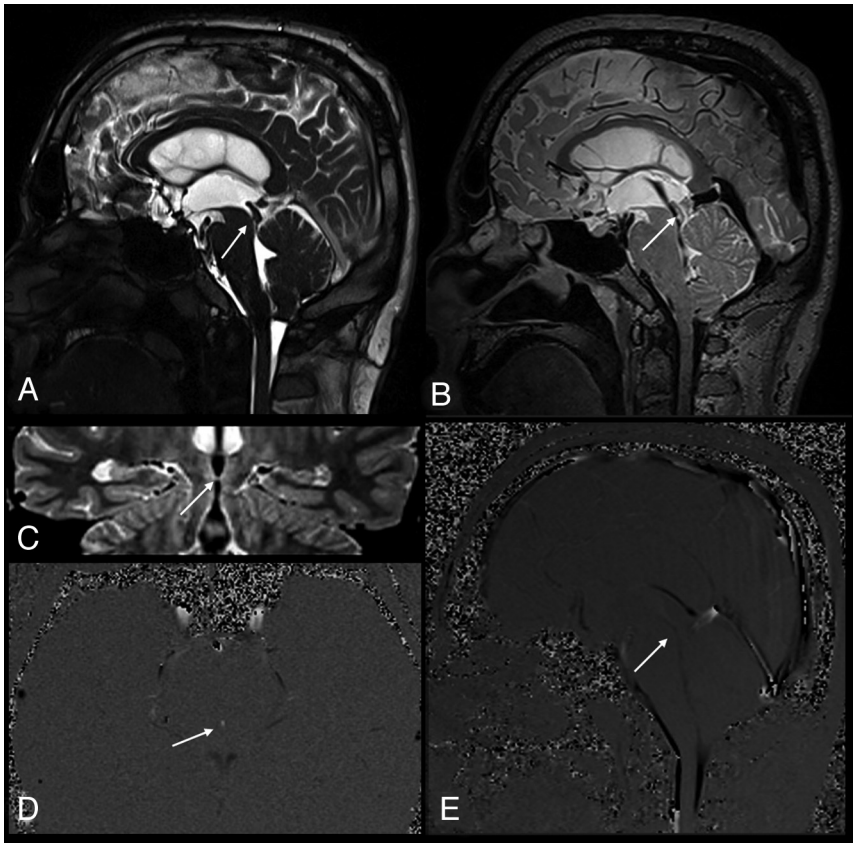

Fig 2. A 35-year-old man with partial aqueductal stenosis (patient 12). *A,* Sagittal T2-weighted image shows a narrowed aqueduct (*arrow*). *B,* Sagittal 3D-SPACE with VFAM image clearly demonstrates a prominent hypointense signal intensity in the cerebral aqueduct (*arrow*). The hypointense signal intensity (also called flow-void sign) on the 3D-SPACE MR image indicates the absence of a complete stenosis. *C,* Coronal oblique curved reconstructed 3D-SPACE image demonstrates a narrow but open aqueduct (*arrow*). *D* and *E,* Axial (*D*) and sagittal (*E*) PC-MRI indicate a narrowed but open aqueduct, consistent with partial aqueductal stenosis (*arrows*).

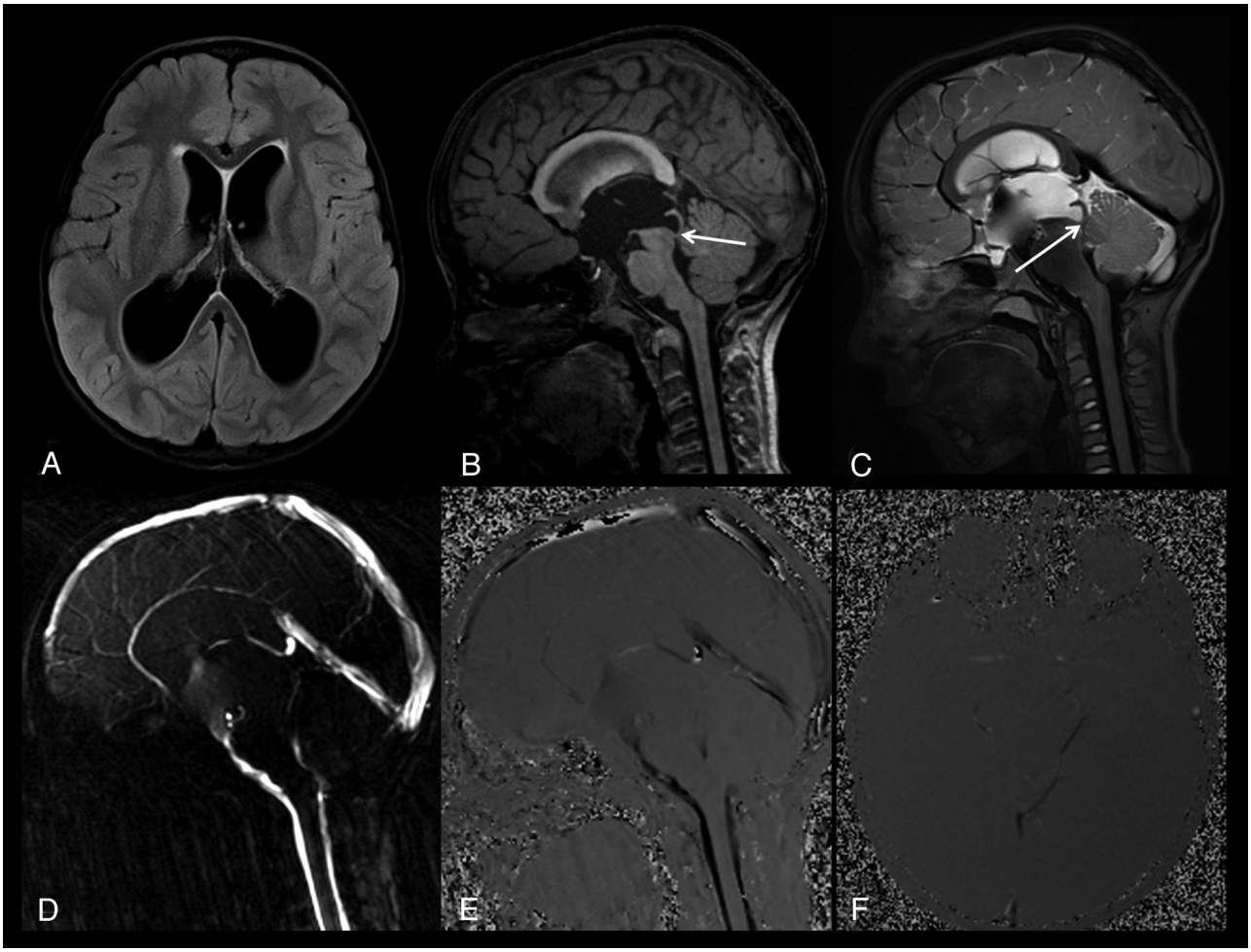

Fig 3. A 7-year-old boy with a complete aqueductal stenosis and hydrocephalus (patient 1). *A*, Axial FLAIR image shows a compensated hydrocephalus. *B*, Sagittal thin-section T1-weighted image demonstrates a narrowed distal aqueduct and a prestenotic aqueductal dilation (*arrow*). *C*, Sagittal 3D-SPACE with VFAM MR image shows a restricted hyperintense CSF flow proximal to the stenotic segment, whereas the unrestricted flow of CSF distal to the stenosis appears hypointense (*arrow*). Sagittal (*D* and *E*) and axial (*F*) PC-MRI shows a complete aqueductal stenosis, consistent with 3D-SPACE images.

Score One (Partial or Suspected Stenosis). The aqueduct has been narrowed, and/or aqueductal flow is barely visible.

Score Two (AS-Positive). The aqueductal lumen is occluded, and/or there is a dilation in the proximal aqueduct (due to web or adhesion). There is no hypointense flow through the aqueduct on 3D-SPACE images.

Both readers were unblinded to the MR pulse sequence type, and in case of discordance between the scores provided by 2 readers, the final decision was determined on a consensus-based evaluation.

Following scoring of 3D-SPACE sequences, both neuroradiologists determined PC-MRI scores. During this evaluation, 3D-SPACE sequences were not included but PC-MRI images were evaluated together with T1-weighted and T2-weighted TSE MR images. After initial evaluations, disagreements about final decisions were resolved by consensus evaluation of the 2 radiologists. During this evaluation, AS patency was scored as described in a prior study.[3]

Score Zero (AS-Negative). Aqueductal CSF flow is clearly visible on all PC-MRI.

Score One (Partial or Suspected AS). The amount of aqueductal flow is decreased. Aqueductal flow can barely be recognized and cannot be observed during whole cardiac cycles.

Score Two (AS-Positive). CSF flow is not visible on all PC-MRI.

After defining the 3D-SPACE and PC-MRI scores according to the above-mentioned information, all sequences were re-evaluated and the consensus-based scores were determined. In this evaluation if there was no AS, the score was 0; if there was a suspicious finding or partial stenosis, the score was 1; and if there was complete AS, the score was recorded as 2. PC-MRI and 3D-SPACE scorings were statistically compared with final consensus scores.

Statistical Analysis

Statistical analyses were performed with the Statistical Package for the Social Sciences software, Version 13.0 (SPSS, Chicago, Illinois). Age values of the patient group were reported with means and SDs. For age values, the concordance of the data to normal distribution was evaluated with the Kolmogorov-Smirnov test. An independent-samples *t* test was performed to compare the values of age variables between sex groups. The agreement level for each type of sequence and consensus-based results was evaluated by using the κ coefficient, which normally ranges between zero and 1. Zero shows that the correlation is a coincidence; a value of 1, on the other hand, is evidence of a perfect correlation. Although κ coefficients should be interpreted within the clinical context, <0.20 was interpreted as poor agreement;

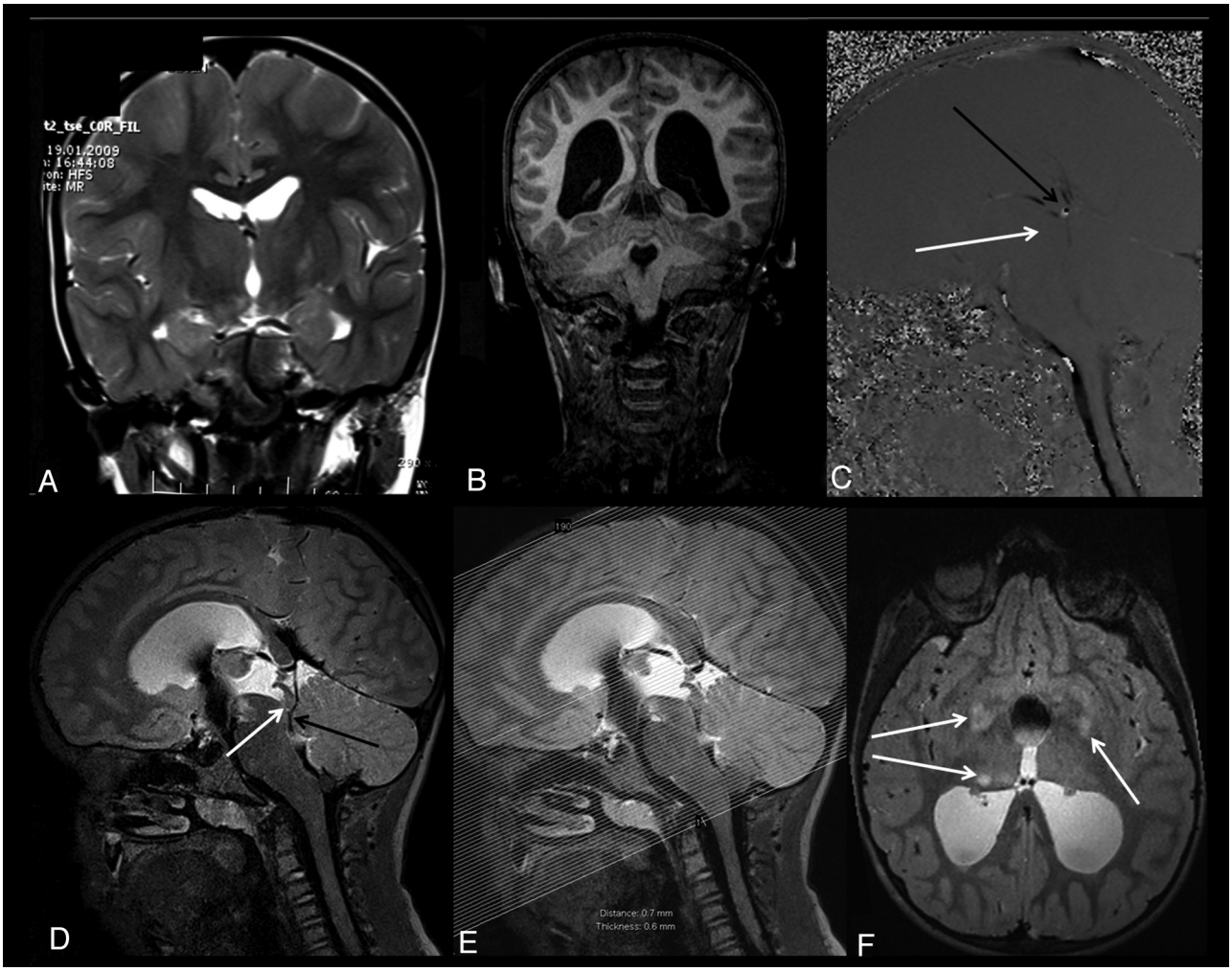

Fig 4. A 9-year-old boy with complete aqueductal stenosis and neurofibromatosis type 1 (patient 21). *A* and *B*, Coronal T2-weighted MR image obtained 2 years ago shows no evidence of hydrocephalus (*A*), whereas a recent T1-weighted MR image shows a progressive hydrocephalus (*B*). *C*, Sagittal PC-MRI obtained at the level of the aqueduct shows absence of aqueductal flow (*white arrow*). Sagittal PC-MRI shows a flow representing the deep venous system in the posteroinferior part of the aqueduct (*black arrow, C*). The pulsation secondary to the venous flow in the quadrigeminal cistern can mimic the aqueductal flow. *D*, Sagittal 3D-SPACE with VFAM MR image clearly demonstrates the venous structures located in the third ventricular outlet–the quadrigeminal cistern (*black arrow*). This image demonstrates a complete aqueductal stenosis (*white arrow, D*). *E* and *F*, Axial thin-section (1 mm) reformatted images obtained from sagittal 3D-SPACE images (*E*) show multiple hamartomas (*arrows, F*).

0.21–0.40, as fair agreement; 0.41–0.60, as moderate agreement; 0.61–0.80, as good agreement; and 0.81–1.00, as very good agreement.[14] To determine the relationship among PC-MRI, SPACE, and consensus-based results, correlation analysis was performed and the Spearman correlation coefficient was also computed. The level of statistically significant difference was $P < .05$.

Results

Demographic data, clinical findings, etiology of hydrocephalus, and MR imaging scores are summarized in Table 1. In all subjects of the control group, a normal aqueductal CSF flow was detected on both PC-MRI and SPACE MR images (grade 0) (Fig 1). Aqueductal width was within normal ranges in all control group subjects without evidence of intra- or periaqueductal pathology.

Statistical analysis of the study population scores revealed an excellent correlation between 3D-SPACE and PC-MRI scores ($\kappa = 0.828$) (Table 2 and Figs 2–4). Similarly, there was an excellent correlation between PC-MRI and consensus-based scores ($r = 0.966$ and $P < .001$) and SPACE and consensus-based scores ($r = 1$ and $P < .001$).

Four patients underwent VPS, whereas 1 had endoscopic third ventriculostomy. In 2 of these 5 patients, early postoperative CT scans revealed regression of hydrocephalus, whereas the remaining 3 patients underwent clinical follow-up, or surgery was planned for them.

Discussion

Diagnosis of AS and periaqueductal abnormalities by routine MR imaging is challenging for neuroradiologists.[3] Routine MR imaging criteria for AS (such as anterior or inferior bulging of the third ventricle and triventricular dilation) are usually subjective and less reproducible without validated cutoff values.[1-3] The criterion standard technique for the diagnosis of obstructive hydrocephalus and AS is ventriculographic studies, and these studies are very invasive and difficult to perform in routine daily practice.[6] CE-MRC is a less invasive morphologic and functional technique for diagnosis of obstructive

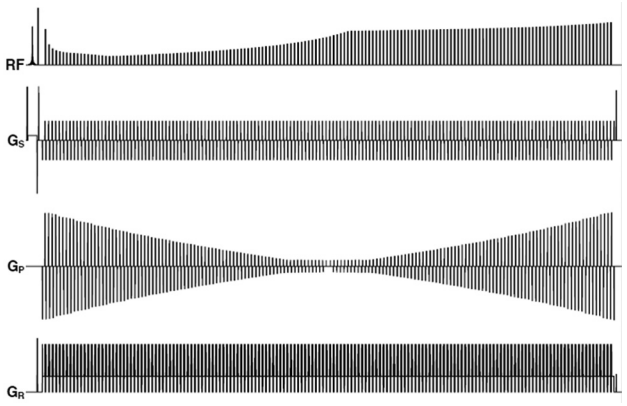

Fig 5. Timing diagram of the 3D-SPACE with different flip angles (3D-SPACE with VFAM). The diagram shows 1 TR of the pulse sequence. The first line shows the variation in the heights of the radio-frequency pulses during the echo-train. G_s is the section-selection gradient, which varies to select different sections in *k*-space. G_k and G_r are the phase-encoding and readout gradients, respectively. The timing diagram was drawn by John P. Mugler III and modified with his permission.

hydrocephalus, and it includes intrathecal administration of gadolinium-diethylene-triamine pentaacetic acid, which is safe but not accepted worldwide.[15-18] In addition to these techniques, PC-MRI and heavily T2-weighted (such as 3D-CISS) or thin-section T2-weighted sequences can be used as alternatives.[3,6,16] However, these techniques have their own advantages and disadvantages.[5,19,20] For instance, PC-MRI can provide physiologic information about CSF flow; however, it might fail in case of complex flow or vascular pulsations.[16] 3D-CISS can give high anatomic resolution, but it cannot provide physiologic information about the aqueductal flow.[6,16] Moreover, in many patients with a prediagnosis of AS, repeated further evaluation with MR imaging may needed, and this increases costs and delays the treatment.

3D-SPACE is a recently developed T2-weighted MR imaging technique that allows an all-in-1 evaluation of the cranium with a single image acquisition (Fig 5). With this flexible sequence; T1-weighted, T2-weighted, proton-attenuation, or FLAIR images can be obtained.[20] The advantages of the 3D-SPACE sequence in evaluation of the spine, pelvis, and abdomen have been reported previously.[8,12] 3D-SPACE sequence uses different flip angles, which enable a low specific absorption rate value, therefore obtaining good T2-weighted images.[8-12] Additionally, thin-sectioned images with good spatial resolution can be obtained in a reasonable acquisition time by using parallel acquisition techniques.[8]

In the current study, we have developed a simpler and more robust approach with T2-weighted 3D-SPACE with VFAM for the diagnosis of obstructive hydrocephalus and AS. To the best of our knowledge, there is no previous report on the role of 3D-SPACE in AS. In our study, we showed that 3D-SPACE with VFAM could provide all the information about CSF flow dynamics with a single-station image acquisition. In this sequence, restricted CSF proximal to the obstruction appeared hyperintense, and freely floating unrestricted CSF was observed as a hypointense signal intensity. 3D-SPACE with VFAM provides noninvasive evaluation of CSF hydrodynamics similar to that in PC-MRI. In addition, it can give all the morphologic information that can be obtained from other sequences in high resolution. Those features of 3D-SPACE are a great advantages for evaluation of AS and obstructive hydrocephalus. Moreover, the sequence can be applied in 3D; the achieved multiplanar reformatted images with high resolution will probably increase the comfort level for the radiologist during the image interpretation. The SPACE sequence with 3D acquisition can supply standardization of MR imaging protocol in patients with AS and/or obstructive hydrocephalus. Another advantage of 3D-SPACE is its capability to decrease MR imaging examination time significantly. Usually T2-weighted and PC-MRI sequences are needed in multiple planes for the evaluation of hydrocephalus. However, 3D-SPACE could supply the same morphologic and physiologic information alone. This would shorten MR imaging examination time by 10 minutes.

There were a few limitations in our study. First, we could not compare the results of 3D-SPACE sequence with a criterion standard ground truth because there was no existing noninvasive criterion standard test and the ethical rules did not allow us to use invasive tests in our study. Second, the observers in our study were not blinded to the MR imaging sequence type during interpretation and comparison. Finally, our patient population was relatively small; therefore, new large-scale studies are needed in this topic.

Conclusions

Diagnosing and defining the etiology of AS are extremely important for accurate therapy planning for hydrocephalus. The 3D-SPACE sequence with VFAM can be used as an efficient single technique in the evaluation of the patients with a prediagnosis of AS because it can supply morphologic as well as physiologic information. With this technique, one can evaluate patients with a prediagnosis of obstructive hydrocephalus in a shorter image-acquisition time and more accurately. 3D-SPACE with VFAM can be useful for optimizing and standardizing the MR imaging protocol of patients with AS.

Acknowledgments

The authors thank Prof. Dr. Ergin Atalar, the director of National MR research center (UMRAM), for the opportunity he provided for 3T MR acquisitions and gratefully acknowledge Prof. Dr. Halil Arslan, John P. Mugler III, Gokhan Ocakoglu, Volkan Acikel, Prof. Dr. Mustafa Karaoglanoglu, Prof. Dr. Ihsan Solaroglu, and Prof. Dr. Faik Ozveren, Dr. Evrim Ozmen, and Dr. Filiz Eryilmaz for their contributions.

References

1. Allan R, Chaseling R, Graf N, et al. **Aqueduct stenosis-benign?** *J Clin Neurosci* 2005;12:178–82
2. Tisell M. **How should primary aqueductal stenosis in adults be treated? A review.** *Acta Neuro Scand* 2005;111:143–53
3. Algin O, Hakyemez B, Parlak M. **Phase-contrast MRI and 3D-CISS versus contrast-enhanced MR cisternography on the evaluation of the aqueductal stenosis.** *Neuroradiology* 2010;52:99–108
4. Sekerci Z, Akalan N, Kilic C, et al. **Primary non-neoplastic aqueductal stenosis associated with Von Recklinghausen's disease.** *Turk Neurosurg* 1989;1:30–33
5. Algin O. **Role of complex hydrocephalus in unsuccessful endoscopic third ventriculostomy.** *Childs Nerv Syst* 2010;26:3–4
6. Algin O, Hakyemez B, Parlak M. **Phase-contrast MRI and 3D-CISS versus contrast-enhanced MR cisternography on the evaluation of spontaneous third ventriculostomy existence.** *J Neuroradiol* 2010;38:98–104
7. Yadav YR, Mukerji G, Parihar V, et al. **Complex hydrocephalus (combination of communicating and obstructive type): an important cause of failed endoscopic third ventriculostomy.** *BMC Res Notes* 2009;2:137

8. Haystead CM, Dale BM, Merkle EM. **N/2 ghosting artifacts: elimination at 3.0-T MR cholangiography with SPACE pulse sequence.** *Radiology* 2008;246: 589–95
9. Mugler JP 3rd, Wald LL, Brookeman JR. **T2-weighted 3D spin-echo train imaging of the brain at 3Tesla: reduced power deposition using low flip-angle refocusing RF pulses.** In: *Proceedings of the International Society for Magnetic Resonance in Medicine,* Scotland, UK. April 21–27, 2001
10. Bink A, Schmitt M, Gaa J, et al. **Detection of lesions in multiple sclerosis by 2D FLAIR and single-slab 3D FLAIR sequences at 3.0 T: initial results.** *Eur Radiol* 2006;16:1104–10
11. Mugler JP 3rd, Menzel MI, Horger W, et al. **High-resolution, multi-contrast 3D imaging of the brain in 15 minutes.** In: *Proceedings of the International Society for Magnetic Resonance in Medicine,* Miami Beach, Florida. May 7–13, 2005
12. Proscia N, Jaffe TA, Neville AM, et al. **MRI of the pelvis in women: 3D versus 2D T2-weighted technique.** *AJR Am J Roentgenol* 2010;195:254–59
13. Oto C, Ekim O, Algin O, et al. **3 Tesla magnetic resonance imaging and multiplanar reconstruction of the brain and its associated structures in pig.** *Ankara Univ Vet Fak Derg* 2011;58:73–78
14. Altman DG. *Practical Statistics for Medical Research*. London, UK: Chapman and Hall; 1991
15. Algin O, Hakyemez B, Gokalp G, et al. **The contribution of 3D-CISS and contrast-enhanced MR cisternography in detecting cerebrospinal fluid leak in patients with rhinorrhoea.** *Br J Radiol* 2010;83:225–32
16. Algin O, Hakyemez B, Gokalp G, et al. **Phase-contrast cine MRI versus MR cisternography on the evaluation of the communication between intraventricular arachnoid cysts and neighbouring cerebrospinal fluid spaces.** *Neuroradiology* 2009;51:305–12
17. Algin O, Hakyemez B, Ocakoglu G, et al. **MR cisternography: is it useful in the diagnosis of normal pressure hydrocephalus and the selection of "good shunt responders"?** *Diagn Interv Radiol* 2011;17:105–11
18. Algin O, Taskapilioglu O, Zan E, et al. **Detection of CSF leaks with magnetic resonance imaging in intracranial hypotension syndrome.** *J Neuroradiol* 2011; 38:175–77. Epub 2011 Jan 6
19. Algin O. **Role of aqueductal CSF stroke volume in idiopathic normal-pressure hydrocephalus.** *AJNR Am J Neuroradiol.* 2010;31:E26–27
20. Watanabe Y, Makidono A, Nakamura M, et al. **3D MR cisternography to identify distal dural rings: comparison of 3D-CISS and 3D-SPACE sequences.** *Magn Reson Med Sci* 2011;10:29–32